The Journal of Experimental Biology 211, 2123-2133
Published by The Company of Biologists 2008
doi:10.1242/jeb.019125

Front leg movements and tibial motoneurons underlying auditory steering in the cricket (*Gryllus bimaculatus* deGeer)

T. Baden and B. Hedwig*
Department of Zoology, University of Cambridge, Downing Street, Cambridge CB2 3EJ, UK
*Author for correspondence (e-mail: bh202@cam.ac.uk)

Accepted 14 April 2008

SUMMARY

Front leg movements in the cricket (*Gryllus bimaculatus*) were measured during phonotactic steering on a trackball together with electromyogram recordings of the tibial extensor and flexor muscles. Up–down leg movements clearly indicated the step cycle and were independent of auditory stimulation. By contrast, left–right movements of the front leg were dependent on sound direction, with crickets performing rapid steering leg movements towards the active speaker. Steering movements were dependent on the phase of sound relative to the step cycle, and were greatest for sounds occurring during the swing phase. During phonotaxis the slow extensor tibiae motoneuron responded to ipsilateral sounds with a latency of 35–40 ms, whereas the fast flexor tibiae motoneurons were excited by contralateral sound. We made intracellular recordings of two tibial extensor and at least eight flexor motoneurons. The fast extensor tibiae, the slow extensor tibiae and one fast flexor tibiae motoneurons were individually identifiable, but a group of at least four fast flexor tibiae as well as at least three slow flexor tibiae motoneurons of highly similar morphology could not be distinguished. Motoneurons received descending inputs from cephalic ganglia and from local prothoracic networks. There was no overlap between the dendritic fields of the tibial motoneurons and the auditory neuropile. They did not respond to auditory stimulation at rest. Neither extracellular stimulation of descending pathways nor pharmacological activation of prothoracic motor networks changed the auditory responsiveness. Therefore, any auditory input to tibial motoneurons is likely to be indirect, possibly *via* the brain.

Key words: cricket, phonotaxis, motoneuron, auditory processing.

INTRODUCTION

Female crickets (*Gryllus bimaculatus*) walk towards singing males. This requires the female to recognise the species specific calling song and consequently steer towards the singer. This behaviour has been studied in great detail at both behavioural and neurobiological levels (e.g. Weber and Thorson 1989; Ball et al., 1989; Schildberger et al., 1989; Pollack, 2001). The auditory afferents transmit the auditory information from the ears located in the front legs to a small number of auditory interneurons in the prothoracic auditory neuropiles. The auditory information is then passed on by few ascending neurons to local and descending brain neurons which may form a pattern recognition network (Schildberger, 1984).

Little is known about the motor performance during phonotaxis, especially upon changes in sound direction. Trackball recordings show that phonotactically walking females turn towards attractive sounds with a delay of 55–60 ms (Hedwig and Poulet, 2004; Hedwig and Poulet, 2005). Pollack and Hoy (Pollack and Hoy, 1980) reported a clear response of a flight muscle to acoustic stimulation during phonotaxis in flying crickets (*Teleogryllus oceanicus*). During both phonotactic flying (Pollack and Hoy, 1980; Nolen and Hoy, 1986; Brodfuehrer and Hoy, 1989) and walking (Poulet and Hedwig, 2005) steering responses may be achieved by a pattern recognition system regulating the gain of a more direct auditory-to-motor loop to the steering motor network. In phonotactically active animals it should therefore be possible to observe specific motor outputs as a direct result of auditory stimulation.

An effective method for steering during walking (Dürr and Ebeling, 2005; Rosano and Webb, 2007) and jumping (Santer et al., 2005) in insects is to change the positioning of the front legs. To identify movement components and consequently motoneurons mediating auditory steering responses we therefore first analysed the movement of a front leg tibia during phonotaxis, and related this to the direction of the sound patterns presented. This identified a critical involvement of front leg movements, and in particular of tibial extension and flexion movements, in auditory steering. Using electromyogram recordings we then analysed the activity of the tibial extensor and flexor motoneurons during phonotaxis. Based on behavioural data and electromyogram recordings from tibial muscles, we identified these intracellular motoneurons and investigated if any direct or indirect auditory input exists and if it can be gated by descending interneurons or local pharmacological stimulation.

MATERIALS AND METHODS

Animals

Female crickets (*Gryllus bimaculatus*) with intact front legs were selected from the colony kept at the Department of Zoology, University of Cambridge, UK, maintained on a 12 h:12 h L:D photocycle. Prior to dissection animals were cold anaesthetised at 4°C for 15 mins. All experiments were performed at room temperature (21–23°C).

Trackball system

For phonotaxis experiments crickets were placed on top of a trackball system and held by a small metal pin waxed onto their back. For details see Hedwig and Poulet (Hedwig and Poulet, 2005).

Optical measurements of leg movements

A custom-build optoelectronic system was used to measure front leg movements (Hedwig, 2000; Hedwig and Becher, 1998). A modified SLR camera with a 2D photodiode (United Detector Technology, Hawthorne, CA, USA; PIN DLS-20) in the plane of the film was used to record the movements of a small piece of reflective material (Scotchlite 7610; 3M Laboratories, Neuss, Germany) fastened around the distal part of the tibia using a small drop of beeswax. We recorded the frontal projection of left tibial movements during walking; i.e. its left–right and up–down movements. This required animals to walk towards the light source of the optical recording system, which reduced the phonotactic performance, even when long wavelength (LED at 630 nm) illumination was used (N=28).

For relating electromyogram (EMG) recordings to the step cycle the forward–backward motion of the femur was recorded from above the animal and used as an indication of the swing and stance phase. Here a one-dimensional version of the optoelectronic system (Laser Components, Olching, Germany; Type 1L30) was used with infrared illumination (LED at 850 nm; N=4).

Acoustic stimulation

An artificial calling song at a carrier frequency of 4.8 kHz, syllable duration of 21 ms, syllable period of 42 ms, chirp duration of 250 ms and chirp period of 500 ms was used (Thorson et al., 1982). Crickets were presented with alternating six-chirp sequences from the left and the right at 75 dB sound pressure level (SPL) relative to 2×10^{-5} Pa. Sound stimuli were digitally generated at 22.05 kHz sampling rate (CoolEdit 2000, now: Adobe Audition; Syntrillium, Phoenix, USA) and were presented by PC audio boards *via* two active speakers (SRS A57; Sony, Tokyo, Japan) positioned 60 cm frontal to the cricket each at an angle of 45° to the animal's length axis. Sound intensities were calibrated with an accuracy of 1 dB at the position of the cricket using a Bruel and Kjaer (Naerum, Denmark) free field microphone (Type 4191) and measuring amplifier (Type 2610).

Electromyogram recordings

Electromyograms (EMG) of tibial extensor and flexor muscles were obtained using two varnish-coated steel wires (30 μm diameter) inserted distally into the extensor tibia muscle or proximally into the flexor tibiae muscles (Fig. 4A). Large amplitude extensor muscle potentials were recorded while at the same time activity in the flexor muscles was reliably picked up at lower amplitude. This occurred *vice versa* in flexor recordings (Fig. 4B). In all further recordings we consequently used this cross talk to identify flexor activity in extensor recordings, avoiding the need for separate flexor recordings. A gliding length filter (Hedwig and Knepper, 1992; Römer et al., 2002) was applied to EMG recordings and EMG peaks were sorted by amplitude of voltage change over time into four classes (Fig. 4C). Signals were picked up using an amplifier (Differential AC Amplifier Model 1700; A-M Systems, Sequim, WA, USA).

Intracellular recordings

For intracellular recordings animals were pinned in a bed of Plasticine™. After a dorsal incision of the thorax the gut was removed and the prothoracic ganglion was exposed. The thoracic cavity was filled with insect saline (140 mmol l^{-1} NaCl, 10 mmol l^{-1} KCl, 4 mmol l^{-1} $CaCl_2$, 4 mmol l^{-1} $NaHCO_3$, 6 mmol l^{-1} NaH_2PO_4). A small metal platform with an optic fibre embedded in it was placed underneath the ganglion. The optic fibre was used for bright-field illumination of the ganglion. The connectives towards the mesothoracic ganglion were cut.

Thick-walled borosilicate micropipettes with resistances of 60–120 MΩ, filled with 5% Lucifer Yellow (Molecular Probes, Eugene, OR, USA) in water (tip) and 1 mol l^{-1} LiCl (shaft) were used to record from the main neurites of motoneurons. Recordings lasted for up to 1 h. For intracellular staining with Lucifer Yellow a 1–9 nA hyperpolarising current was injected for 5–20 mins. Signals were recorded using an SEC-10L amplifier (NPI, Tamm, Germany) and digitised at 10 kHz. Motoneurons were characterised and identified according to morphology, the impact of spiking on tibial movement and the size of evoked EMG potentials. A total of ~250 crickets were used, of which 93 yielded the presented data.

Sensory stimulation during intracellular recordings

Auditory

Sound stimuli were presented using a small speaker (ø=2 cm) attached to the wide end of a 15 cm conical copper tube, the narrow end of which was placed 2 cm from the opening of the ipsilateral auditory spiracle. Intensities of stimuli were calibrated to an accuracy of 0.5 dB SPL at the position of the spiracle. The carrier frequency of sound stimuli was 4.8 kHz, and the amplitude used throughout was 90 dB SPL. Background noise in the room was <45 dB SPL.

Air currents

Air currents stimuli were generated using a Picopump (PV 820 Pneumatic PicoPump; WPI, Sarasota, FL, USA) connected to a rubber tube (i.d. 0.5 mm), the other end of which was positioned 5 cm in front of the animal.

Tactile

Tactile stimuli were applied manually using a small paintbrush. In all recordings the tibia and tarsus were gently touched at several positions, and the largest response recorded.

Visual

Visual stimuli were generated using a white LED (Nichia 1100 mcd, 50° divergent angle; Tokushima, Japan) positioned at a distance of 3 cm from the head of the animal pointing at the eye ipsilateral to the front leg investigated.

Activation of descending pathways

A small bipolar hook electrode was placed underneath the connective ipsilateral to the recorded motoneuron between the prothoracic and suboesophageal ganglia and insulated with a mixture of 90% Vaseline™ and 10% paraffin. Stimuli were generated using a stimulus isolation unit (WPI A360 SIU), triggered by a custom-built pulse generator. Current pulses were of 2 ms duration and between 1 and 50 μA amplitude, applied at 1–100 Hz (N=19).

Pharmacological stimulation

To disinhibit or activate thoracic motor networks the ganglion was bathed in the GABA blocker picrotoxin (10^{-4} mol l^{-1} in saline) or the muscarinic receptor agonist pilocarpine (10^{-3} mol l^{-1} in saline), respectively (Ryckebusch and Laurent, 1993). This elicited increased motor activity after 20–30 s, which persisted until the entire thoracic cavity was washed with saline. To ensure all activity recorded was generated within the prothoracic ganglion, the connectives towards the suboesophageal ganglion were cut in N=3/23 experiments.

Processing of neurons stained with Lucifer Yellow

After intracellular staining of a motoneuron it was left for 5–20 mins to allow the dye to diffuse throughout the cell. The ganglion was

then dissected and placed in 4% formaldehyde for 1 h. The specimens were then dehydrated and cleared in methyl salicylate (Sigma-Aldrich, St Louis, MO, USA). The ganglion was photographed using a digital SLR camera (Canon EOS 350D) attached to a Zeiss (Axiophot) fluorescence microscope with a ultraviolet light source (Zeiss VHW 50f-2b). For graphical projections of neural arborisations photo-stacks were traced manually using Adobe Photoshop (CS 8.00).

Data sampling and analysis

An A/D board (MIO 16E4, National Instruments, Austin, TX, USA) linked to custom-built software running under LabView 5.01 (National Instruments) was used in all experiments. Behavioural and electrophysiological data was analysed in Neurolab (Hedwig and Knepper, 1992). Further data analysis was performed using MatLab 6.5 (Mathworks, Natick, MA, USA).

RESULTS

Front leg movements during phonotaxis

Animals walking on the trackball responded to sequences of six chirps alternating from the left and the right with steering towards the active speaker (Fig. 1A, top). The optoelectronic system picked up the up–down and left–right movements of the left front leg. Up–down movements revealed the stepping cycle, with rapid movements indicating swing phase, and slower movements indicating stance. Small amplitude oscillations in the trackball recording also copied the step pattern. Up–down leg movements were unaffected by the sound direction. By contrast, the pattern of the left–right movements changed with the direction of acoustic stimulation (Fig. 1A, bottom). When steering towards the ipsilateral (left) speaker left–right movements were small and corresponded to left–right movements during straight ahead walking. When animals steered towards the contralateral (right) speaker left–right leg movements were clearly larger, extending to the right towards the direction of acoustic stimulation. These movement patterns were remarkably constant during steering to either side, but upon a change in direction of acoustic stimulation leg movement patterns were switched within a single step cycle (Fig. 1A,B). To better illustrate the rapid effect of change in sound direction on left–right leg movements in Fig. 1B the movement pattern before the turn (red) is superimposed on the leg movement trace during a turn as indicated. After less than 60 ms after ipsilateral sound presentation the recorded movement trace deviates from the expected movement. From the up–down and left–right leg movement components we obtained two-dimensional projections of the average movement pattern of the front leg at the position of the reflective disk (Fig. 1C). This revealed that during steering to the contralateral, but not during steering to the ipsilateral side, the leg reached in front of the head during swing phase in order to pull the animal towards the stimulated side during the following stance.

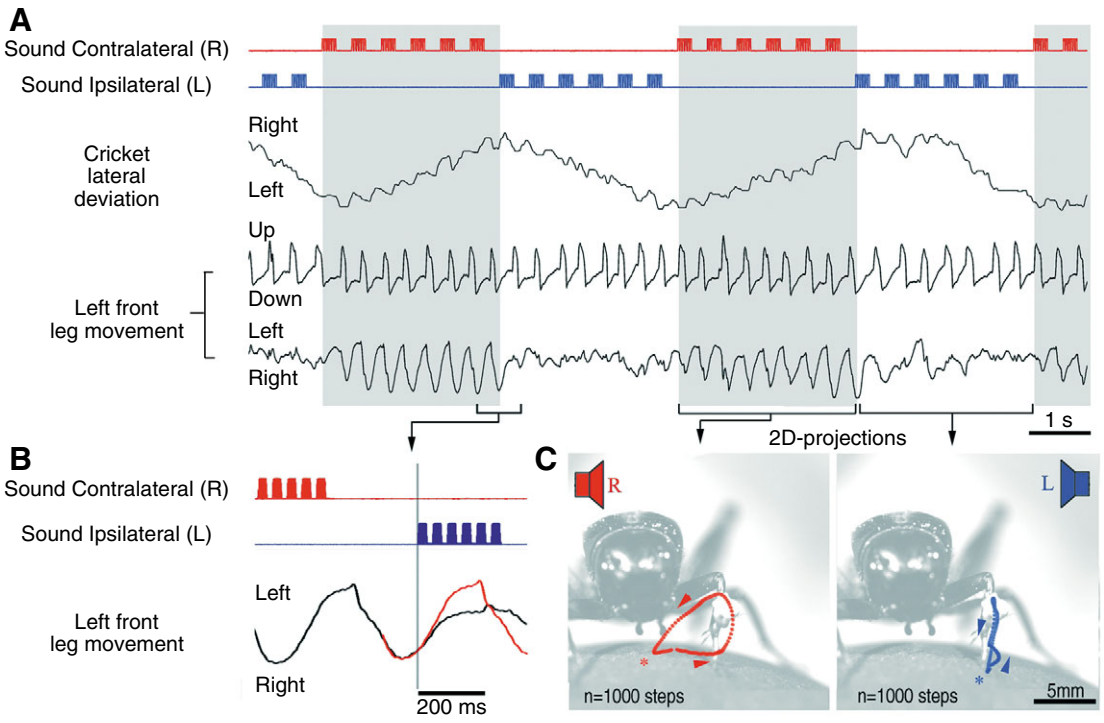

Fig. 1. Movements of the left front leg during phonotaxis. (A) Animals responded to alternating six-chirp sequences from the left and right with steering towards the active speaker. During steering to the contralateral (right) speaker the left front leg performed large left–right movements towards the stimulated side, but during steering to the ipsilateral (left) speaker only small left–right movements occurred. The pattern of up–down leg movements was constant. (B) Rapid change in leg movement; section from A as indicated. The red trace is an exact copy of the first step shown, indicating the leg movement without a turn. Within two syllables of ipsilateral sound presentation (60 ms) the movement deviates from the predicted trace. (C) Up–down and left–right recordings of left front leg movements during steering were combined into 2D projections. The background photograph was taken independently for illustrative purposes. During steering to the contralateral (right) speaker the anterior extreme point (AEP, asterisk) of the left front leg was shifted in front of the head during the swing phase. This allowed animals to pull towards the active speaker during the following stance phase. By contrast, during steering to the ipsilateral (left) speaker the AEP was directly in front of the leg resting position.

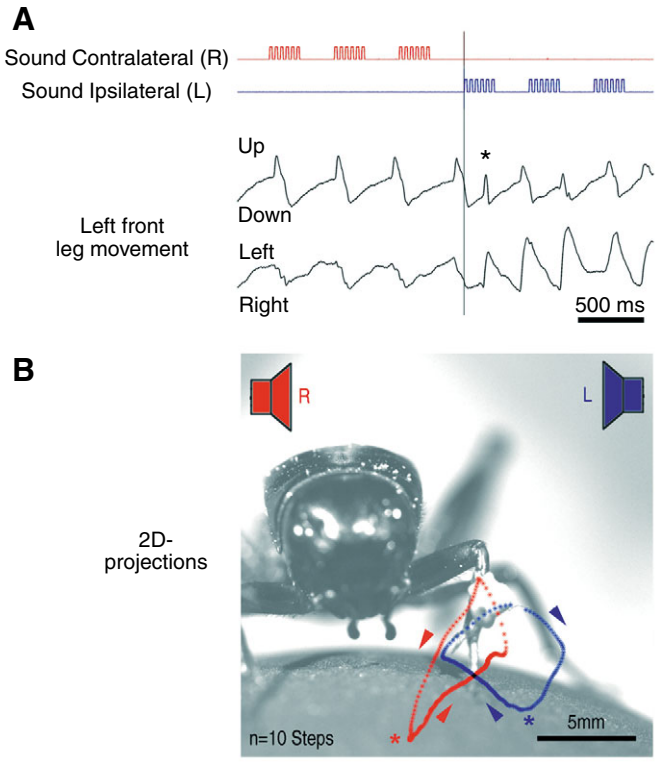

Fig. 2. Bilateral steering movements of the left front leg. (A) A third of animals exhibited strong steering movements of the front leg towards both ipsilateral and contralateral acoustic stimulation. In less than 10% of cases the step rhythm was disrupted during a turn (asterisk). (B) Two-dimensional projections of up–down and left–right movement components of the left front leg. The AEP (asterisk) was shifted towards the respective active speaker during both contralateral (right) and ipsilateral (left) sound presentation. This allowed the animal to pull towards the active speaker during the following stance phase for both ipsilateral and contralateral steering.

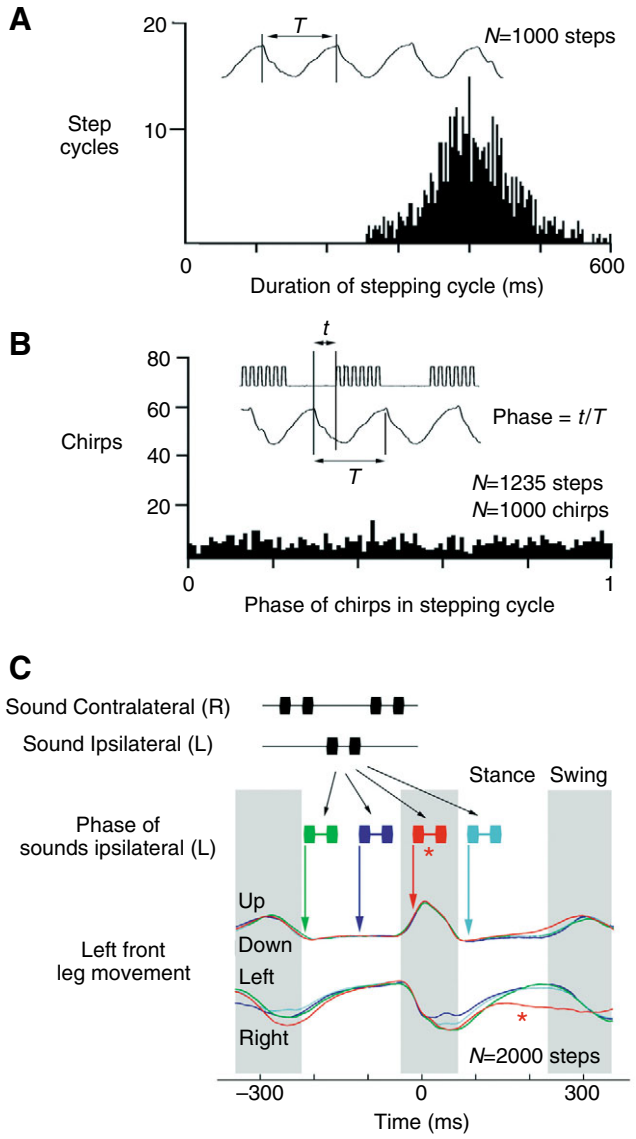

Fig. 3. Phase relations between step and sound rhythms. (A) Interval histogram of step cycle durations ranging between 250 and 600 ms, with a mean of 396 ms. (B) Phase diagram of chirps within the step cycle. This revealed no indication that the step cycle was coupled to the chirp pattern. (C) Double pulse paradigm with the first and last two syllables of a chirp presented from contralateral (right), but the middle two syllables presented from ipsilateral (left) speakers (top traces). Stepping cycles were sorted into 20 bins according to the phase values of acoustic stimulation; only four bins are shown for clarity. Only when the ipsilateral two syllables occurred during swing phase, were left–right front leg movements smaller in the following stance phase (asterisk).

A third of animals showed large left–right leg movements also towards ipsilateral (left) sounds. Here the tibia moved away from the body during swing phase and towards the body during stance (Fig. 2). Furthermore in less than 10% of cases turning disturbed the step rhythm (Fig. 2A, asterisk).

It may be advantageous for phonotactic steering to synchronise the stepping cycle with the rhythm of incoming chirps (Hedwig and Poulet, 2004). Step cycle durations ranged between 250 ms and 600 ms (21–23°C). Fig. 3A shows the distribution of step cycle durations for one representative animal. We tested animals with chirp rates between 1 and 5 Hz. There was no coupling between the step rhythm and the chirp rhythm at any repetition rate tested when the sound direction was constant (Fig. 3B). We furthermore tested if there is a phase-dependent effect of incoming sounds on the leg movements using a double pulse paradigm, where the first and last two syllables of each chirp were presented from contralateral speaker, and the middle two syllables from ipsilateral speaker (Fig. 3C inset). The leg movement traces were sorted into 20 bins depending on their phase relative to the onset of the ipsilateral sound, and averaged within each bin, centred at the peak of swing phase (t=0 ms). Leg movement traces from four representative phase relations between ipsilateral sounds presentation and the step cycle are shown (Fig. 3C). Ipsilateral acoustic stimulation during swing phase, but not during stance, reduced the amplitude of the left–right leg movement during the following step (red, asterisk).

Movements in at least three joints can contribute to the measured movements of the front leg. However, owing to the nature of our recording method we cannot directly identify the contribution of coxal rotations, tibial extension and flexion movements or overall bending movements of the body to the observed front leg movement patterns (see Discussion).

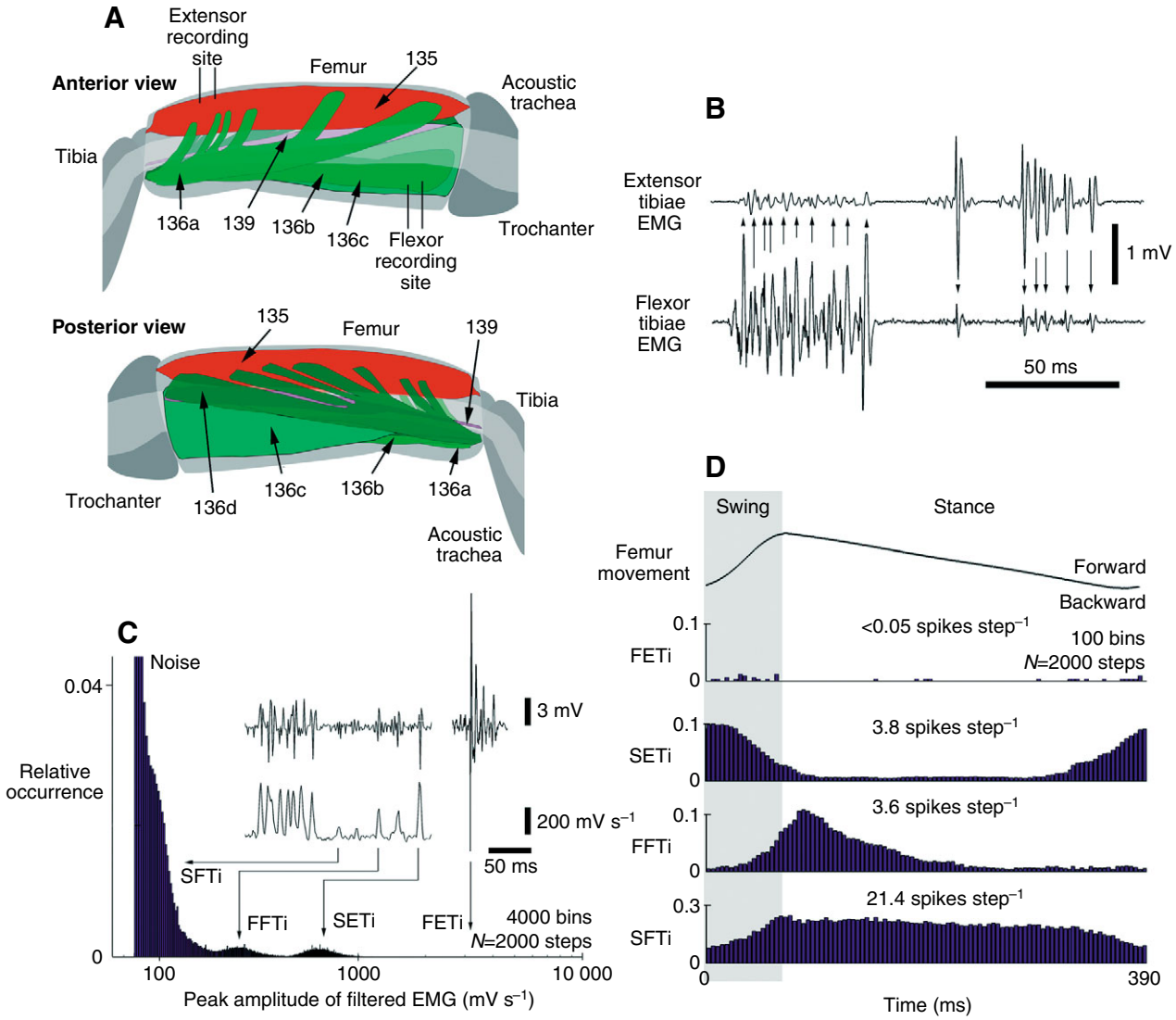

Fig. 4. Tibial muscles and EMG recordings during walking. (A) A single tibia extensor muscle (red, 135) extends dorsally throughout the entire length of the femur. Four tibia flexor muscle bundles (green, 136a–d) were located ventrally. A retractor unguis (pink, 139) runs anteriorly along the acoustic trachea. (B) Simultaneous tibial extensor and tibial flexor EMG recordings were taken at positions as indicated in A. Large amplitude muscle potentials recorded in the extensor were directly related to small amplitude muscle potentials measured in the flexor, and *vice versa*. (C) Amplitude histogram of gliding length filtered tibial extensor EMG recording of a walking cricket. Four different motor units were clearly identified. A muscle potential attributed to FETi is shown only in the EMG recording because of its large amplitude. FETi spikes occurred very rarely during walking (1 in 20 steps) and are not visible in the histogram. (D) EMG recordings were obtained during walking, with simultaneous recordings of forward-backward movements of the femur as an indication of the step cycle. Peaks of the EMGs were sorted according to amplitudes: FETi>SETi>FFTi>SFTi. The occurrence of motor unit activity within each step was normalised to the mean duration of steps (390 ms).

Tibial musculature

To investigate the control of tibial movements we identified the tibial musculature and its innervation. Nomenclature was based on the description of the hind leg musculature in locust (Snodgrass, 1929). A single tibial extensor muscle (dorsal: 135) and four tibial flexor muscle bundles (one antero-ventral, two ventral, one postero-ventral: 136a–d) were identified (Fig. 4A). The proximal ends of flexors 136a and 136d attached to multiple points along the anterior and posterior cuticle, respectively. A single retractor unguis (139) was positioned antero-dorsal to the acoustic trachea.

EMG recordings during phonotaxis

Extracellular recordings from tibial muscles were used to monitor tibial motoneuron activity. A single pair of EMG electrodes inserted into the extensor muscle made it possible to monitor both extensor and flexor muscle potentials (see Materials and methods). We recorded the muscle activity during walking and simultaneously measured forward–backward movements of the femur to monitor the step cycle. Amplitude sorting of gliding length filtered (see Materials and methods) EMG potentials allowed us to separate at least four different motor units contributing to tibial movements during walking (Fig. 4C). These were characterised by their typical activity during walking. The description of EMG activity presented in this paragraph relates to motor units. An intracellular identification of the associated motoneurons is presented below. Fig. 4D shows the average spike occurrence of each motor unit during the step cycle. Fast extensor tibiae (FETi) activity was present in less than 1 out of 20 steps and occurred just prior, or during, early swing

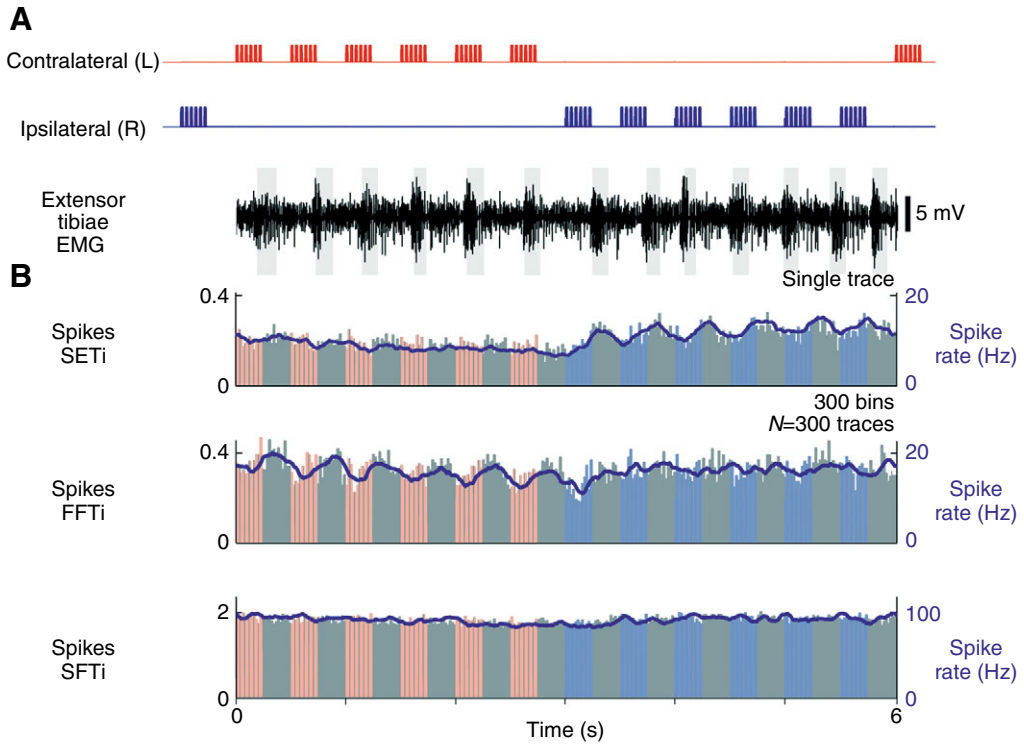

Fig. 5. EMG recordings during phonotaxis. (A) Alternating six-chirp sequences from the left and right were related to right front extensor tibiae EMG traces while animals were acoustically orienting on a trackball. In single trace EMG recordings the step pattern was the dominant modulation in motor unit activity. (B) Averaging EMG activity with respect to the start of the contralateral sound pattern revealed the auditory input to tibial motoneurons. SETi spike rate increased in response to ipsilateral (right) sound, and FFTi spike rate was modulated by contralateral (left) sound. SFTi activity was unaffected. The spike rate of FETi was too low to reveal any auditory activation and is not presented.

phase. This motor unit only showed increased activity (1–2 spikes per step) during escape running, elicited by wind stimulation of the cerci. Slow extensor tibiae (SETi) activity also occurred just prior and during early swing phase. Fast flexor tibiae (FFTi) potentials occurred during late swing and early stance phase. Finally, slow flexor tibiae (SFTi) activity was high throughout the step cycle, but reduced just prior and during early swing phase.

We next analysed the effect of acoustic stimulation on the spike activity of the tibial extensor and flexor motor units during phonotactic steering (Fig. 5). In single-trial recordings motor unit activity in the step rhythm was dominant and masked any effects of acoustic stimulation (Fig. 5A). We therefore averaged the discharge rate of motor units relative to the cycle of the sound pattern, thereby discarding the effect of the step rhythm (Fig. 5B). This revealed clear modulations of SETi and FFTi motor activity in response to acoustic stimulation: each chirp presented from the ipsilateral (blue) position gave rise to a distinct increase in SETi activity, whereas each contralateral chirp (red) increased FFTi activity. SETi and FFTi only responded to acoustic stimulation during phonotaxis and not in standing or non-acoustically orienting animals, indicating a clear phonotaxis-dependent steering response. SFTi and FETi were unaffected by the sounds. To investigate the delay between sound presentation and evoked spike activity in SETi we presented animals with the double pulse paradigm (Fig. 6). The trackball recording revealed clear lateral steering movements towards the active speaker with a delay of 55–60 ms, consistent with previous findings (Hedwig and Poulet, 2004). Increases in SETi activity always preceded changes in the trackball movements, and reliably increased with a delay of 35–40 ms after ipsilateral sound presentation.

Recordings of front leg movement patterns and analysis of tibial EMG activity during auditory steering therefore clearly highlight the importance of tibial motor control in mediating phonotactic behaviour.

Identification of tibial motoneurons

To identify the motoneurons underlying tibial EMG activity during phonotactic walking, we intracellularly recorded and identified the front leg tibial motoneurons and revealed their morphology and synaptic inputs. Identification criteria included the effect of depolarisation on tibial movement, the amplitude of the elicited EMG signal and their morphology.

Two extensor tibiae motoneurons, the FETi and the SETi (Fig. 7A), were individually identified. Each spike of the FETi elicited a >10 mV EMG potential and gave rise to a rapid tibial extension. By contrast, SETi spikes gave rise to 3–5 mV EMG potentials and resulted in slower, graded extension movements, dependent on spike rate. One fast flexor motoneuron (FFTi) was also identified (Fig. 7B left). In addition a group of at least four FFTi motoneurons was morphologically distinct from the latter FFTi (Fig. 7B right) and a group of at least three SFTi motoneurons (Fig. 7C) were distinguished. The minimal number given for these groups of FFTi and SFTi are derived from sequential stainings of the respective neuron type in the same specimen. The single identifiable FFTi was labelled FFTi1 and the morphologically distinct group of four FFTi was labelled FFTi2–5 (Fig. 7B). Spike activity in either type of FFTi gave rise to 2–3 mV EMG potentials and resulted in graded flexion movements of the tibia. SFTi spikes elicited the smallest (1 mV) EMG potentials, and alone were insufficient to move the tibia.

Both FETi and SETi EMG potentials recorded during phonotaxis could be clearly attributed to their corresponding individually identified motoneurons. FFTi EMG potentials may be the result of either FFTi1 or FFTi2–5 motoneuron activity. SFTi EMG activity was attributed to the group of SFTi1–3 motoneurons.

Morphology of tibial motoneurons

Somata of all motoneurons were located antero-ventrally with the somata of SETi, FETi and the group of FFTi2–5 typically adjoining

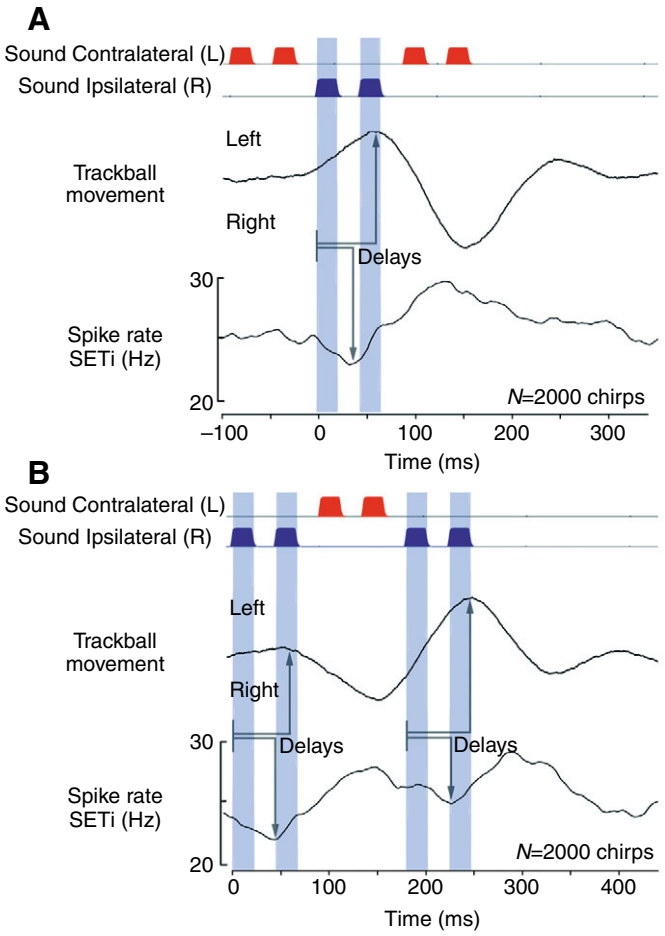

Fig. 6. Timing of auditory inputs to SETi. (A,B) Animals acoustically orienting on the trackball were presented with the double pulse paradigm. The trackball recording revealed steering towards the stimulated side with a delay of 55–60 ms. Simultaneously recorded EMG traces reveal an increase in SETi activity with a delay of 35–40 ms after ipsilateral (right) sound presentation.

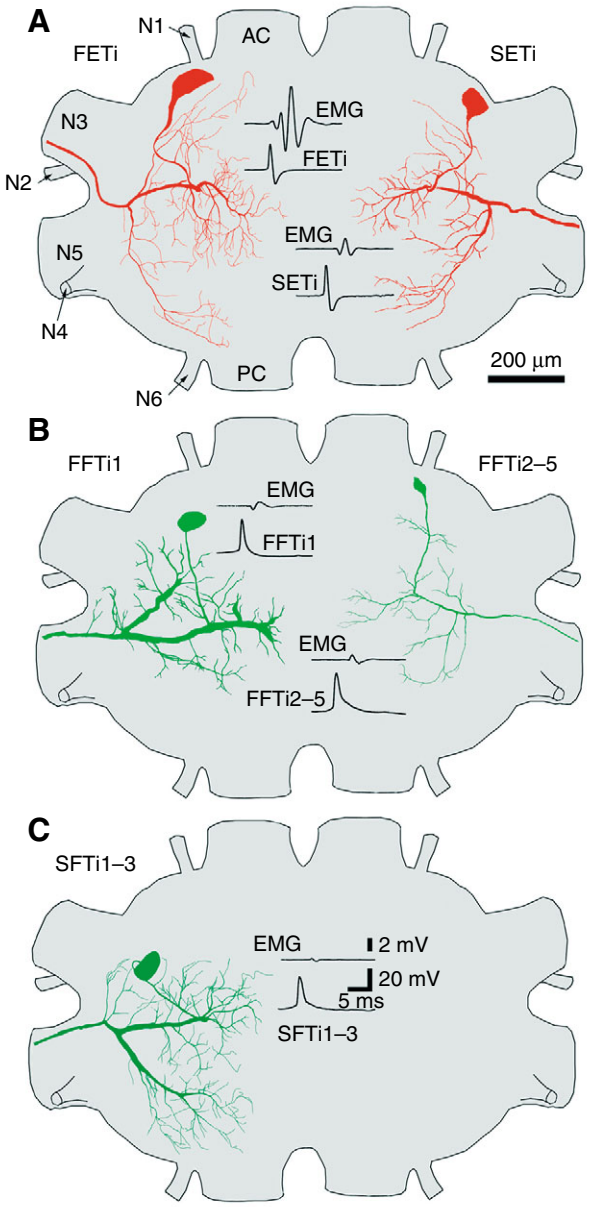

Fig. 7. Morphology of tibial motoneurons. Motoneurons were located dorsally in the prothoracic ganglion, with ventral somata. The amplitude of EMG potentials elicited by spikes in each respective motoneuron is indicated. (A) Structure of the FETi (*N*=12 stainings) and SETi (*N*=28). (B) Structure of the FFTi1 (*N*=6) and the FFTi2–5 (*N*=12). (C) Example of a SFTi1–3 (*N*=15). The projection patterns of the main neurites varied between SFTi motoneurons, but the soma position and the overall dendritic field was very similar.

the anterior-most border of the ganglion, whereas somata of the group of SFTi1–3 and that of FFTi1 were located more posteriorly. The most prominent neurite of all motoneurons runs 150–200 µm beneath the dorsal surface of the ganglion between the midline and the point where the axon left the ganglion through the respective side nerve. A second large neurite runs posteriorly in all motoneurons except for FFTi1, where it runs antero-medially. All motoneurons exit the ganglion *via* nerve 5, with exception of the FETi which exits *via* nerve 3 (Fig. 7A left).

The dendrites of both FETi and SETi extend throughout the entire ipsilateral dorsal surface of the ganglion, with extensive medial branching (Fig. 7A). The main processes and the posterior dendrite of SETi were thicker than those of FETi. The main processes of FFTi1 were very large (ø=20–30 µm), with the main, thickest neurite almost reaching the midline. The main branches gave off very short secondary neurites (Fig. 7B left). By contrast, the main neurites of FFTi2–5 (Fig. 7B right) were much thinner (ø=5 µm) than of any other tibial motoneuron, with secondary and tertiary branching patterns similar to the extensor motoneurons, but very sparse. The morphology of the main neurites of SFTi1–3 varied substantially and only one example is given (Fig. 7C). The extent of the branching patterns of their secondary and tertiary neurites was similar to SETi. None of the motoneurons exhibited any overlap with the ventrally located auditory neuropile (Schildberger et al., 1989; Imaizumi and Pollack, 2005).

Sensory and central inputs to tibial motoneurons

Sensory inputs to tibial motoneurons were investigated during rest and activity. SETi, FETi and FFTi2–5 did not spike at rest. By contrast, SFTi1–3 and FFTi1 were active with a spike rate between 0.5–2 Hz and generated frequent excitatory and inhibitory postsynaptic potential (EPSPs and IPSPs; Fig. 8A) in resting animals. We did not detect any auditory or visual inputs in this state.

However, all neurons received both wind and tactile inputs (Fig. 8B), also demonstrating that auditory evoked responses were unlikely to have been missed because of a lack of sensitivity of the recordings. Only tactile inputs to SFTi1–3 could elicit spikes.

Thoracic motoneurons frequently receive inputs from descending interneurons of the brain (Burrows, 1996). Previous studies suggested that the brain may be involved in auditory pattern recognition (Schildberger, 1984): successful recognition of species-specific song may lead to phonotactic steering by a descending pathway acting on the thoracic motor system (Poulet and Hedwig, 2005; Pollack and Hoy, 1980). To reveal any descending control over tibial motoneuron activity we extracellularly stimulated the ipsilateral descending connective between the prothoracic and the suboesophageal ganglia. This allowed us to elicit EPSPs and spikes in all tibial motoneurons (Fig. 8C). EPSPs occurred with a delay of <3 ms and were dependent on the amplitude of the stimulation current, indicative of a direct, parallel polyneural input from descending pathways.

During walking, leg motoneurons are under the control of local central pattern generating networks (Burrows, 1996, Büschges et al., 2008). We therefore tested for local prothoracic inputs to tibial motoneurons. Prothoracic motor networks were pharmacologically activated by the muscarinic receptor agonist pilocarpine (10^{-3} mol l^{-1}) or the GABA antagonist picrotoxin

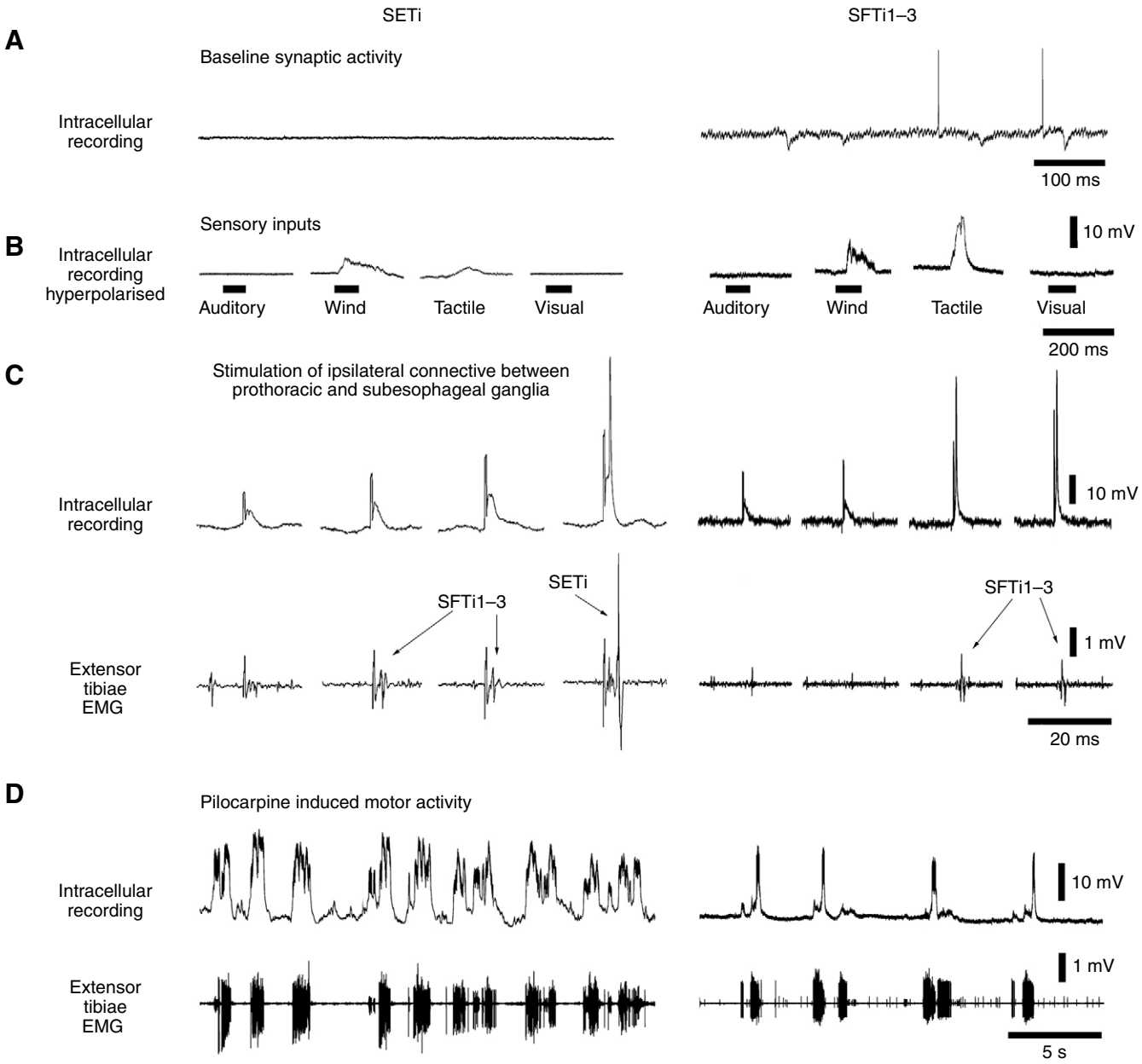

Fig. 8. Sensory and central inputs to tibial motoneurons. (A) Intracellular recordings of SETi (left) and SFTi1–3 (right) at rest. No synaptic activity was recorded in SETi, while SFTi1–3 received frequent synaptic inputs. (B) Sensory stimulation during hyperpolarising current injection to unmask any weak inputs. Motoneurons at rest did not respond to auditory or visual inputs, but did respond to wind and tactile inputs. (C) Extracellular electrical stimulation of descending pathways evoked EPSPs and spikes in all motoneurons. Four examples are shown of recordings with increasing stimulation amplitude. (D) Bath application of pilocarpine or picrotoxin elicited motor bursts in all motoneurons.

(10^{-4} mol l^{-1}) (Ryckebusch and Laurent, 1993; Büschges et al., 1995). In all motoneurons both picrotoxin and pilocarpine elicited powerful motor bursts that exceeded spike threshold. However, bursts were irregular and occurred at lower frequency (0.1–1 Hz) than during walking (2–3 Hz; Fig. 8D). This experiment demonstrated inputs to all tibial motoneurons from prothoracic motor networks.

Can auditory inputs be gated?

Our data from EMG recordings during phonotaxis demonstrate an auditory input to SETi and to at least one of the two groups of FFTi motoneurons. However, we did not detect any auditory inputs to these motoneurons at rest. Poulet and Hedwig (Poulet and Hedwig, 2005) suggested a descending modulatory pathway, which may gate auditory inputs towards the motor system in phonotactically active animals. It may therefore be possible to unmask auditory inputs to SETi or either class of FFTi by stimulating descending pathways. A strong hyperpolarising current (5 nA) was injected into SETi to both prevent spiking and reveal potentially weak auditory inputs during and after stimulation of the connectives. However, neither single trial nor continuous activation of descending pathways upregulated any putative auditory inputs to any of the tibial motoneurons (Fig. 9A). Furthermore no auditory responses were apparent during pharmacologically elicited motor activity (Fig. 9B). The trace presented is a section between ongoing motor activity and was chosen as it lacks motor burst activity that could obscure any auditory inputs.

DISCUSSION

It was the aim of this study to investigate the role of front leg movements during phonotactic steering in crickets. We furthermore aimed to identify the underlying neuronal control over tibial movements at the level of the tibial muscles, the tibial motoneurons and the sensory and central control over these motoneurons. We also set out to identify or unmask any auditory inputs towards the motor system, as required for phonotactic steering.

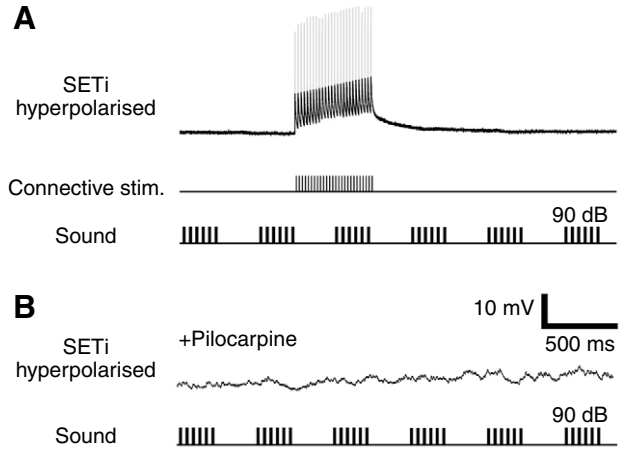

Fig. 9. Can auditory inputs be gated? Intracellular recordings of SETi during stimulation of descending pathways (A) and during pharmacologically elicited motor activity using pilocarpine (B) or picrotoxin (not shown). Chirps (4.8 kHz 90 dB) were presented at 2 Hz repetition rate. Neither stimulation of descending pathways nor pharmacological manipulation gated any auditory inputs to SETi. In both cases a hyperpolarising current (5 nA) was injected to reveal even small inputs.

Front leg movements during phonotaxis

We studied front leg movements during phonotaxis in order to identify the motor pathway involved in phonotactic steering. During forward walking left–right front leg movements were remarkably small, but during steering leg movements showed a clear dependency on sound direction (Figs 1, 2). Throughout stimulation from either left or right, steering movements were unchanged (Fig. 1A, Fig. 2A), however, in response to a change in sound direction animals switched the steering pattern within a single step cycle, and frequently after less than ~60 ms (Fig. 1B, Fig. 2A). This remarkably fast response is in agreement with rapid steering movements of 55–60 ms measured with a trackball system (Hedwig and Poulet, 2004; Hedwig and Poulet, 2005) and indicates the importance of the front legs in steering.

There are three possible, non-exclusive modes of steering using the front legs: (1) changing the femoral/tibial angle (Dürr and Ebeling, 2005), (2) changing the positioning of the femur (Laurent and Richard, 1986a; Laurent and Richard, 1986b; Dürr and Ebeling, 2005), and (3) overall bending movements of the prothoracic segment passively moving the front legs into a steering position (unlike in many species of grasshoppers or phasmids, the prothoracic segment of cricket is not rigidly connected to the mesothorax and could be used in steering). Although effects due to positioning of the femur and bending of the prothoracic segment are superimposed on the tibial movements due to the nature of our recording technique, we judge these effects as less significant: during visual inspection of front leg steering movements, tibial extension and flexion movements could clearly be identified. Detailed analysis of leg positioning using high-speed video analysis did clearly demonstrate the contribution of tibial extension and flexion movements in steering (A. Witney and B.H., unpublished data).

Movement in the femoral-tibial joint provides a powerful way to affect the movement direction of the animal: increased tibial extensions shift the anterior end point (AEP) towards a more extreme position along the axis of the femur and therefore allow consequent tibial flexion to pull the animal towards that point. For tibial movements to allow for steering, the overall step cycle must be taken into account: whereas an extension during swing phase will shift the AEP forwards, an activation of extensor motoneurons during stance will push the animal away from the AEP, resulting in a sideways or even backwards movement of the cricket. Similarly flexion during swing phase would decrease the step size and therefore limit the steering, whereas flexion during stance would pull the animal forwards, towards the AEP. High speed video recordings will be necessary to clarify the details of sound-induced leg steering movements.

During acoustic stimulation, animals did not couple their overall step rhythm to the chirp rhythm (Fig. 3B). This is in contrast to locust flight pattern generators, which are under pivotal control of rhythmic wind inputs to synchronise wing beats between animals (e.g. Camhi et el., 1995). The absence of coupling between sounds and the step cycle in crickets indicated that here steering commands are probably integrated with the walking central pattern generator (CPG). They do not modify the overall stepping pattern, but instead modulate the amplitude of steering responses. The phase dependency of motor effects caused by sounds during swing phase supports this.

Anatomy and morphology

The muscles of the front leg tibia and their innervation patterns showed several parallels to that of the locust front leg (Hoyle, 1955a; Hoyle, 1955b), stick insect middle leg (Bässler, 1993) and the cricket middle leg (Nishino, 2003). The single large extensor muscle was

driven by two excitatory extensor motoneurons, a FETi and a SETi. These corresponded to tibial extensor motoneurons in cricket and locust hind legs and stick insect middle legs. The flexor system was more complex, but acted as a single functional unit because of a common distal attachment point. At least eight excitatory flexor motoneurons exit. The cricket hind leg tibia is innervated by at least 19, the locust hind leg by nine and the stick insect by 14 excitatory flexor motoneurons. All motoneurons identified, except for the FETi, which projected its axon through nerve III, projected their axons through nerve V. This corresponds to the arrangement of the front tibial motoneurons in locusts (Burrows, 1996).

EMG recordings

We investigated the role of the tibial extensor motoneurons and flexor motor units in walking and phonotactic steering. During walking, tibial extensions were carried almost entirely by SETi. By contrast, SFTi was tonically active throughout stance phase but reduced activity during swing (Fig. 4D). Flexion was strongly driven by FFTi activity, which peaked at the beginning of stance phase. We did not attempt to identify any common inhibitor motoneurons or dorsal unpaired median cells innervating tibial muscles. In particular the low activity of the tibial extensors is in clear contrast to similar studies performed on locust legs (Burns and Usherwood, 1979) and cockroach hind legs (Krauthamer and Fourtner, 1978) where at high stepping rates SETi is tonically active and bursts of FETi activity support the step rhythm. Because of its very low spike rate during phonotactic walking FETi is unlikely to contribute to steering under normal circumstances. It remains open whether FETi supports steering at very high stepping rates. However, the low SETi activity during walking in *G. bimaculatus* leaves room for its recruitment during steering: SETi responded to ipsilateral acoustic stimulation during phonotaxis. EMG recordings also demonstrate an auditory input to at least one type of FFTi motoneurons (Fig. 5). It is unclear which, if not both types of FFTi motoneurons underlie these auditory responses during phonotaxis. Previously Pollack and Hoy (Pollack and Hoy, 1980) demonstrated activity in dorsal longitudinal muscles in response to individual sound pulses in flying crickets (*Teleogryllus oceanicus*) (see also Nolen and Hoy, 1986). These inputs result in bending of the abdomen towards the direction of the sound during flight. It is, however, unclear to what extent abdominal movements contribute to auditory steering during walking. While these findings emphasise the likely involvement of multiple motor systems of the body other than tibial extension and flexion movements in supporting cricket phonotaxis behaviour, our behavioural experiments highlight both the SETi and either FFTi1 or FFTi2–5 as key output neurons for phonotactic steering during walking.

Auditory control over tibial motoneurons

As demonstrated in EMG recordings tibial motoneurons integrate auditory inputs with activity from walking-pattern-generating networks during phonotactic steering. However, intracellular recordings revealed no auditory inputs to any motoneuron identified at rest or during pharmacologically elicited motor activity. Furthermore, motoneurons were located dorsally and did not extend any neurites towards the ventrally located auditory neuropiles (Schildberger et al., 1989). The auditory input to motoneurons therefore has to be indirect, leaving two options: (1) it may be entirely local, *via* interneurons in the prothoracic ganglion or (2) it may reach motoneurons *via* the brain. In this respect the timing is crucial: increased spike rate in SETi in response to acoustic stimulation during EMG recordings occurred after 35–40 ms. Subtracting 4 ms to allow for spikes to be generated and propagated towards the muscles (Fig. 7) this leaves 31–36 ms for the synaptic input to be evoked in the motoneurons following acoustic stimulation. First order prothoracic auditory interneurons such as the omega 1 neuron (ON1) or ascending neuron 1 (AN1) respond to acoustic stimulation with a latency of 15–17 ms (Wohlers and Huber, 1978). This leaves 14–21 ms for the information to reach motoneurons *via* either a thoracic or a cephalic pathway. This delay is rather long for an entirely prothoracic pathway, but it also leaves only little time for a loop *via* the brain: AN1 activity in the brain occurs with a latency of 20–22 ms (Schildberger, 1984) (M. Zorović, personal communication), implying a propagation time of auditory signals between the prothoracic ganglion and the brain of ~5 ms. Two way propagation to and from the brain therefore costs a total ~10 ms leaving 4–11 ms for local processing in the brain. In support of a cephalic pathway, extracellular stimulation of descending pathways clearly indicated a direct, parallel polyneural descending input to tibial motoneurons. The physiological relevance of the extracellularly evoked synchronous spike activity in several descending axons remains unclear. In addition several multimodal descending brain neurons respond to auditory stimuli and are known to terminate dorsally in all thoracic ganglia (Staudacher, 2001). These respond with latencies between 25–47 ms at the level of the connectives between the suboesophageal and prothoracic ganglia, and may therefore be candidate neurons for a descending auditory control of front tibial motoneurons. Similarly, Brodfuehrer and Hoy (Brodfuehrer and Hoy, 1989; Brodfuehrer and Hoy, 1990) identified several ultrasound-sensitive descending brain neurons of *T. oceanicus* that may mediate negative phonotactic steering responses. An entirely prothoracic auditory loop towards the motoneurons would require descending gating control (Pollack and Hoy, 1980; Poulet and Hedwig, 2005) to enable the pathway only during steering. However, stimulation of descending interneurons did not unmask any auditory inputs to the motoneurons. Furthermore, despite decades of research, no prothoracic auditory interneurons have been identified that project from the ventral auditory neuropiles towards the dorsal motoneurons. Instead the gating mechanism may exist in the brain, with a descending pathway mediating the steering responses. Most of AN1's presynaptic terminals project antero-ventrally in the brain, laterally of the α-lobes (Schildberger, 1984), however, most descending brain neurons extend their dendritic fields in the ventral posterior deutocerebrum (Staudacher, 1998). We therefore anticipate a cephalic auditory loop to require at least two synapses within the brain, involving local brain neurons forwarding the auditory information from AN1 towards descending pathways.

Future experiments will aim at a more comprehensive understanding of auditory processing in the brain. The identification of the descending pathways to the SETi and FFTi motoneurons as well as the postsynaptic targets of AN1 will be crucial. Furthermore, the identification of the mechanism underlying the gating of the auditory-to-motor pathway during phonotaxis is a central question.

LIST OF ABBREVIATIONS

AEP	anterior end point
AN1	ascending neuron 1
CPG	central pattern generator
EMG	electromyogram
EPSP	excitatory postsynaptic potentials
FETi	fast extensor tibiae
FFTi	fast flexor tibiae
GABA	gamma-aminobutyric acid
LED	light emitting diode
ON1	omega 1 neuron

PEP	posterior end point
SETi	slow extensor tibiae
SFTi	slow flexor tibiae
SLR	single-lens reflex
SPL	sound pressure level

We thank Leanne Scott for excellent technical assistance with behavioural experiments and Malcolm Burrows, Maja Zorović and Olivier Faivre for critical reading of the manuscript. This study was supported by the BBSRC, Royal Society and Cambridge University European Trust.

REFERENCES

Ball, E. E., Oldfield, B. P. and Rudolph, K. M. (1989). Auditory organ structure, development, and function. In *Cricket Behaviour and Neurobiology* (ed. F. Huber, T. E. Moore and W. Loher), pp. 391-423. Ithaca, NY: Cornell University Press.

Bässler, U. (1993). The femur-tibia control system of stick insects – a model system for the study of the neural basis of joint control. *Brain Res. Rev.* **18**, 207-226.

Brodfuehrer, P. D. and Hoy, R. R. (1989). Integration of ultrasound and flight inputs on descending neurons in the cricket brain. *J. Exp. Biol.* **145**, 157-171.

Brodfuehrer, P. D. and Hoy, R. R. (1990). Ultrasound sensitive neurons in the cricket brain. *J. Comp. Physiol. A* **166**, 651-662.

Burns, M. D. and Usherwood, P. N. R. (1979). The control of walking in orthoptera. II. Motor neuron activity in normal free-walking animals. *J. Exp. Biol.* **79**, 69-98.

Burrows, M. (1996). Components of the nervous system. In *The Neurobiology of an Insect Brain*, pp. 48-67. New York: Oxford University Press.

Büschges, A., Schmitz, J. and Bässler, U. (1995). Rhythmic patterns in the thoracic nerve cord of the stick insect induced by pilocarpine. *J Exp. Biol.* **198**, 435-456.

Büschges, A., Akay, T., Gabriel, J. P. and Schmidt, J. (2008). Organizing network action for locomotion: Insights from studying insects walking. *Brain Res. Rev.* **57**, 162-171.

Camhi, J., Sumbre, G. and Wendler, G. (1995). Wing-beat coupling between flying locust pairs: preferred phase and lift enhancement. *J. Exp. Biol.* **198**, 1051-1063.

Dürr, V. and Ebeling, W. (2005). The behavioural transition from straight to curve walking: kinetics of leg movement parameters and the initiation of turning. *J. Exp. Biol.* **208**, 2237-2252.

Hedwig, B. (2000). A highly sensitive opto-electronic system for the measurement of movements. *J. Neurosci. Methods* **100**, 165-171.

Hedwig, B. and Becher, G. (1998). Forewing movements and intracellular motoneurons stimulation in tethered flying locusts. *J. Exp. Biol.* **201**, 731-744.

Hedwig, B. and Knepper, M. (1992). NEUROLAB, a comprehensive program for the analysis of neurophysiological and behavioural data. *J. Neurosci. Methods* **45**, 135-148.

Hedwig, B. and Poulet, J. F. A. (2004). Complex auditory behaviour emerges from simple reactive steering. *Nature* **430**, 781-785.

Hedwig, B. and Poulet, J. F. A. (2005). Mechanisms underlying phonotactic steering in the cricket *Gryllus bimaculatus* revealed with a fast trackball system. *J. Exp. Biol.* **208**, 915-927.

Hoyle, G. (1955a). The anatomy and innervation of skeletal muscle. *Proc. R. Soc. Lond. B Biol. Sci.* **143**, 281-343.

Hoyle, G. (1955b). Neuromuscular mechanism of a locust skeletal muscle. *Proc. R. Soc. Lond. B Biol. Sci.* **143**, 343-367.

Imaizumi, K. and Pollack, G. S. (2005). Central projections of auditory receptor of crickets. *J. Comp. Neurol.* **493**, 439-447.

Krauthamer, V. and Fourtner, C. R. (1978). Locomotory activity in the extensor and flexor tibiae of the cockroach, *Periplaneta americana*. *J. Insect Physiol.* **24**, 813-819.

Laurent, G. and Richard, D. (1986a). The organization and role during locomotion of the proximal musculature of the cricket foreleg. I. Anatomy and Innervation. *J. Exp. Biol.* **123**, 255-283.

Laurent, G. and Richard, D. (1986b). The organization and role during locomotion of the proximal musculature of the cricket foreleg. II. Electromyographic activity during stepping patterns. *J. Exp. Biol.* **123**, 285-306.

Nishino, H. (2003). Local innervation patterns of the metathoracic flexor and extensor tibiae motor neurons in the cricket *Gryllus bimaculatus*. *Zool. Sci.* **20**, 697-707.

Nolen, T. G. and Hoy, R. R. (1986). Phonotaxis in flying crickets. I. Attraction to the calling song and avoidance of bat-like ultrasound are discrete behaviors. *J. Comp. Physiol. A* **159**, 423-439.

Pollack, G. S. (2001). Analysis of temporal patterns of communication signals. *Curr. Opin. Neurobiol.* **11**, 734-738.

Pollack, G. S. and Hoy, R. (1980). Phonotaxis in flying crickets: neural correlates. *J. Insect Physiol.* **27**, 41-45.

Poulet, J. F. A. and Hedwig, B. (2005). Auditory orientation in crickets: pattern recognition controls reactive steering. *Proc. Natl. Acad. Sci. USA* **102**, 15665-15669.

Römer, H., Hedwig, B. and Ott, S. R. (2002). Contralateral inhibition as a sensory bias: the neural basis for a female preference in a synchronously calling bushcricket, *Mecopoda elongata*. *Eur. J. Neurosci.* **15**, 1655-1662.

Rosano, H. and Webb, B. (2007). A dynamic model of thoracis differentiation for the control of turning in the stick insect. *Biol. Cybern.* **96**, 229-246.

Ryckebusch, S. and Laurent, G. (1993). Rhythmic patterns evoked in locust leg motor neurons by muscarinic agonist pilocarpine. *J. Neurophysiol.* **69**, 1583-1595.

Santer, R. D., Yamawaki, Y., Rind, F. C. and Simmons, P. J. (2005). Motor activity and trajectory control during escape jumping in the locust *Locusta migratoria*. *J. Comp. Physiol. A* **191**, 965-975.

Schildberger, K. (1984). Temporal selectivity of identified auditory neurons in the cricket brain. *J. Comp. Physiol. A* **155**, 171-185.

Schildberger, K., Huber, F. and Wohlers, D. W. (1989). Central auditory pathway: neuronal correlates of phonotactic behaviour. In *Cricket Behaviour and Neurobiology* (ed. F. Huber, T. E. Moore and W. Loher), pp. 391-423. Ithaca: Cornell University Press.

Snodgrass, R. C. (1929). The thoracic mechanism of a grasshopper and its antecedents. *Smithson. Misc. Collect.* **82**, 1-111.

Staudacher, E. (1998). Distribution and morphology of descending brain neurons in the crickets *Gryllus bimaculatus*. *Cell Tissue Res.* **294**, 187-202.

Staudacher, U. M. (2001). Sensory responses of descending brain neurons in the walking cricket *Gryllus bimaculatus*. *J. Comp. Physiol. A* **187**, 1-17.

Thorson, J., Weber, T. and Huber, F. (1982). Auditory behaviour of the cricket. II. Simplicity of calling-song recognition in *Gryllus*, and anomalous phonotaxis at abnormal carrier frequencies. *J. Comp. Physiol. A* **146**, 361-378.

Weber, T. and Thorson, J. (1989). Phonotactic behaviour of walking crickets. In *Cricket Behaviour and Neurobiology* (ed. F. Huber, T. E. Moore and W. Loher), pp. 310-340. Ithaca: Cornell University Press.

Wohlers, D. W. and Huber, F. (1978). Intracellular recording and staining of cricket auditory interneurons (*Gryllus campestris* L., *Gryllus bimaculatus* DeGeer). *J. Comp. Physiol. A* **127**, 11-28.